Strongly Coupled Single-Phase Flow Problems: Effects of Density Variation, Hydrodynamic Dispersion, and First Order Decay

Curtis M. Oldenburg and Karsten Pruess

Earth Sciences Division, Lawrence Berkeley Laboratory
University of California, Berkeley, CA 94720

ABSTRACT

We have developed TOUGH2 modules for strongly coupled flow and transport that include full hydrodynamic dispersion. T2DM models two-dimensional flow and transport in systems with variable salinity, while T2DMR includes radionuclide transport with first-order decay of a parent-daughter chain of radionuclide components in variable salinity systems. T2DM has been applied to a variety of coupled flow problems including the pure solutal convection problem of Elder and the mixed free and forced convection salt-dome flow problem. In the Elder and salt-dome flow problems, density changes of up to 20% caused by brine concentration variations lead to strong coupling between the velocity and brine concentration fields. T2DM efficiently calculates flow and transport for these problems. We have applied T2DMR to the dispersive transport and decay of radionuclide tracers in flow fields with permeability heterogeneities and recirculating flows. Coupling in these problems occurs by velocity-dependent hydrodynamic dispersion. Our results show that the maximum daughter species concentration may occur fully within a recirculating or low-velocity region. In all of the problems, we observe very efficient handling of the strongly coupled flow and transport processes.

INTRODUCTION

TOUGH2 uses a residual-based convergence criterion and Newton-Raphson iteration to handle the non-linear equations for the changes in primary variables (Pruess, 1987; 1991). This formulation is efficient for handling the strong non-linearities of multiphase flow which enter, for example, through relative permeability, capillary pressure, and density effects. These same techniques also make possible the efficient solution of strongly coupled single-phase flow problems. In this paper, we show results of TOUGH2 calculations for two classic strongly coupled flow problems and we investigate radionuclide decay and hydrodynamic dispersion in a variable velocity flow field. The example problems are solved with T2DM, and T2DMR, the dispersion and radionuclide transport modules for TOUGH2. Complete details of the dispersion model and its implementation are presented in Oldenburg and Pruess (1993; 1994a). The focus of this paper is on model results and the handling of strongly coupled flow problems in the TOUGH2 simulator.

CONVERGENCE CRITERION

The example problems presented here are single-phase flow problems with coupled flow and transport. The coupling between the flow field and the transport equations arises through density effects, hydrodynamic dispersion, and a combination of the two. Coupling is handled in TOUGH2 by a residual-based formulation in which the discretized mass balance equations at each time step are solved simultaneously taking all coupling terms into account. For each grid block n and mass component κ, the residual is defined as $R_n^{(\kappa)}$ = {left-hand side} – {right-hand side} of the space-and-time discretized conservation equations. Specifically, the residual $R_n^{(\kappa)}$ at time step k+1 is written

$$R_n^{(\kappa)k+1} = M_n^{(\kappa)k+1} - M_n^{(\kappa)k} - \frac{\Delta t}{V_n}\left\{\sum_m A_{nm}F_{nm}^{(\kappa)k+1} + V_n\, q_n^{(\kappa)k+1}\right\} \quad (1),$$

where m labels the grid blocks that are connected to n, and $\Delta t = t(k+1) - t(k)$ is the time-step size. Using 2 components (water and brine) with isothermal conditions in EOS7, there are 2N residuals for a flow system with N grid blocks. These 2N residuals are generally non-linear functions of the 2N primary variables, namely, the set of pressures and brine mass fractions. The set of 2N non-linear discretized equations $R_n^{(\kappa)} = 0$ is solved by Newton-Raphson iteration. Expanding to first order in the primary variables and introducing an iteration index p, we have

$$R_n^{(\kappa)k+1}(x_{i,p+1}) = R_n^{(\kappa)k+1}(x_{i,p}) + \sum_i \frac{\partial R_n^{(\kappa)k+1}}{\partial x_i}\Big|_p (x_{i,p+1} - x_{i,p}) \stackrel{!}{=} 0 \quad (2)$$

where $x_{i,p+1}$ is the set of unknown primary variables at time step k+1, iteration level p+1. Solution of Eq. 2 results in an updated estimate of the primary variables. Iteration continues until all residuals are reduced to a small fraction of the accumulation terms, i.e.,

$$\left|\frac{R_{n,p+1}^{(\kappa),k+1}}{M_n^{(\kappa),k+1}}\right| \le \varepsilon \quad (3).$$

The convergence criterion is set to a small number, typically ε = 1.e-5. When the accumulation term is very small, an absolute rather than a relative convergence criterion may be used.

The solution technique in TOUGH2 is efficient for strongly coupled flow problems for two reasons. First, both the flow and transport equations are solved simultaneously, with full coupling between the flow equations (through density), solute concentration, and solute dispersion. In this way, the numerical solution of flow and transport is coupled just as the physical flow and transport are coupled. Because the time-step size can be larger in this coupled solution technique, fewer time steps are needed. Second, reduction of residuals below a small fraction of the mass accumulation term ensures that the difference equations have in fact been solved; there is no possibility for "false" convergence. Other codes often used for coupled single and multiphase flow problems (e.g., FAST (Holzbecher, 1991), HST3D (Kipp, 1987), SUTRA (Voss, 1984), and SWIFT (Reeves et al., 1986)) use a criterion of "small" relative or absolute changes in primary variables to determine convergence. Such a criterion is dangerous in that small changes in primary variables during iteration do not necessarily indicate convergence, but may arise far from convergence when the convergence rate is slow.

DENSITY-COUPLED FLOW

Pure Solutal Free Convection

The Elder problem is a free-convection problem originally conceived as being pure thermal convection with heating from below

(Elder, 1967), but easily adapted for pure solutal convection with a salt source at the top. The large maximum density change (20%) makes this a strongly coupled flow problem. Consistent with the Elder pure thermal convection problem, which was performed in a Hele-Shaw cell, the emphasis in this problem is on the density coupling rather than coupling through hydrodynamic dispersion. Thus, transport is by advection and pure molecular diffusion. In the problem, a body of liquid-saturated porous media is juxtaposed against an infinite source of dense brine above. The domain, boundary conditions, and discretization for the problem are presented in Fig. 1, where symmetry about the line Y = 0 m has been assumed. The parameters for the problem are presented in Table 1.

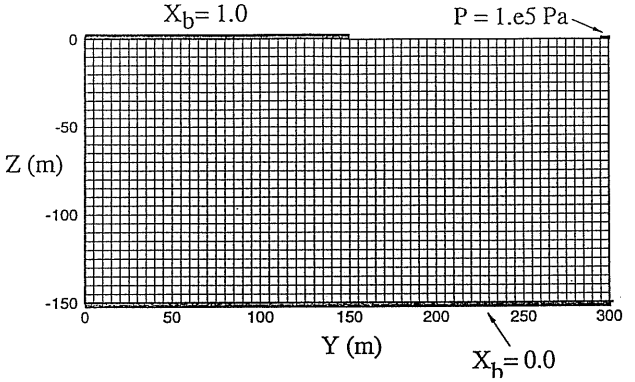

Fig. 1. Domain, boundary conditions, and discretization for the Elder (1967) pure solutal convection problem.

Table 1. Parameters for the Elder (1967) pure solutal convection problem.

symbol	quantity	value	units
ϕ	porosity	.1	–
k	permeability	4.845×10^{-13}	m^2
μ	viscosity	1.0×10^{-3}	Pa s
g.	gravity	9.81	$m\ s^{-2}$
α_T	transverse dispersivity	0.	m
α_L	longitudinal dispersivity	0.	m
d	molecular diffusivity	3.565×10^{-6}	$m^2\ s^{-1}$
τ	tortuosity	1.	–
ρ_0	density of pure water	1000.	$kg\ m^{-3}$
ρ_b	density of pure brine	1200.	$kg\ m^{-3}$

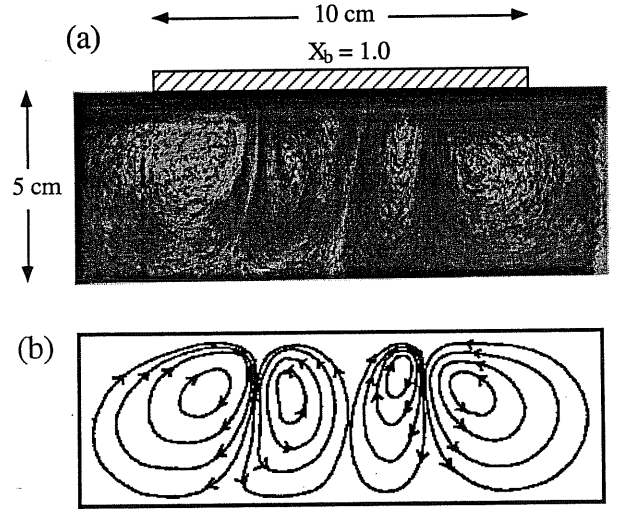

Fig. 2. Experimental results of Elder (1967): (a) flow visualization as presented by Elder (1967) and embellished with brine source boundary condition; (b) approximate streamlines made explicit for clarity.

We show in Fig. 2 a reproduction of a photo from Elder's paper (Elder, 1967), turned upside down to correspond to our solutal convection scenario and embellished with the boundary conditions and approximate streamlines. The photo clearly shows that Elder's laboratory result had the equivalent of central upflow. Fig. 3 shows our corresponding calculated results after 152 time steps at t = 20 years. Our calculated result agrees closely with Elder's experimental result. The convection process begins with downward flow near the right-hand edge of the dense brine region (Fig. 3) where the X_b = 1.0 boundary condition is maintained. Flow is upwards on both sides of this brine plume. With time, this region of downflow moves towards the center line (Y = 0). However, it does not actually reach the center line, and at later times in this transient flow there is upflow at the center line (Y = 0), which corresponds to central upwelling. For discussion and comparison of prior modeling efforts with current results, see Oldenburg and Pruess (1994b, 1995a).

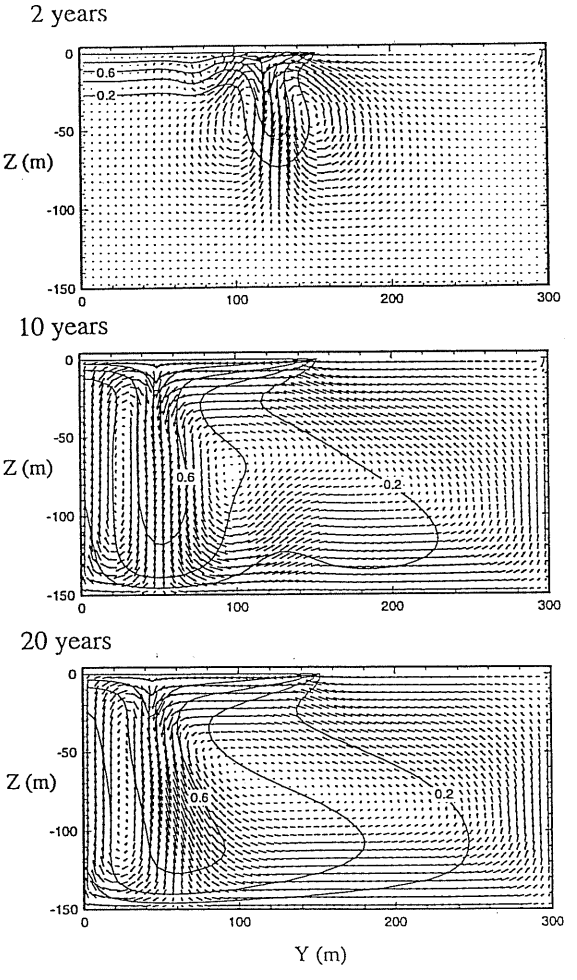

Fig. 3. Results for the Elder free-convection problem at t = 2, 10, and 20 years. Contours are labeled with mass fraction of maximum brine concentration ($X_{b,max}$ = 1.0). Flow field and concentration isopleths show agreement with the experimental results of Elder (1967) reproduced in Fig. 2.

Salt-Dome Flow

Patterned loosely after the hydrogeologic conditions at Gorleben, Germany, a site under consideration for use as a high-level nuclear waste repository (Langer et al., 1991), the salt-dome flow problem was set forth in the Hydrocoin code verification study (Andersson et al., 1986). In the problem, fresh water enters from the top boundary on the left-hand side of a two-dimensional domain, flows past a region of dense brine at the bottom, and then flows out through the top boundary on the right-hand side (Fig. 4). The in-flow and out-flow regions along the top boundary are not defined *a priori*, but must be determined as part of the solution. Transport of

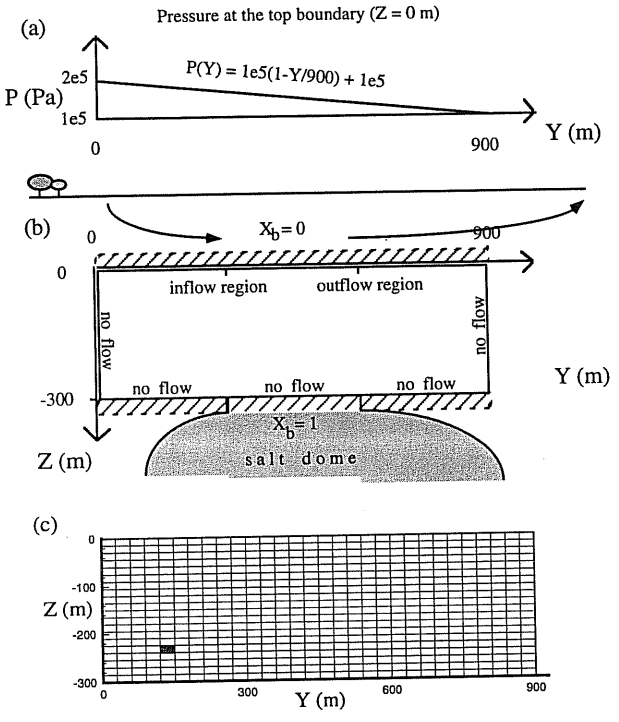

Fig 4. Domain and boundary conditions for the salt-dome flow problem. (a) Top pressure boundary condition. (b) Schematic and boundary conditions of the domain. (c) Discretization.

brine is by advection and hydrodynamic dispersion (no molecular diffusion). Strong coupling occurs through density variations of 20% and through hydrodynamic dispersion. Prior simulation results concluded that the steady-state flow field has a large recirculation in the bottom region, although the strong coupling in the problem has led to great difficulty in achieving steady state solutions (Andersson et al., 1986; Herbert et al., 1988).

Results for the problem calculated with T2DM are shown in Fig. 5. After approximately 100 time steps, these results are very close to steady state as evidenced by time steps on the order of 100 years. Further confirmation of the single steady-state solution was obtained by starting the simulation with different initial conditions and obtaining the same steady state. The calculated results show that fresh water picks up saline brine from the bottom brine boundary by hydrodynamic dispersion. Advection and dispersion then transport the plume of salty water generally from left to right. Our steady-state flow pattern is quite different from results presented by other workers, who obtained large recirculations in what was deemed to be a "steady" state. Based on our results we suggest that the recirculating state found by others is not "steady," but was mistaken as such because previous simulations had employed parameter stepping and a convergence criterion based on (small) changes in the primary variables rather than on residuals. A detailed discussion of these subtle issues is presented in Oldenburg and Pruess (1995a).

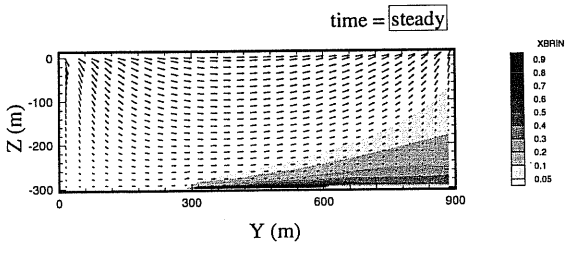

Fig. 5. Steady-state velocity and brine mass fraction for the salt-dome flow problem showing the swept-forward flow pattern. A weak recirculation occurs in the lower right-hand corner.

Table 2. Parameters for the salt-dome flow problem.

symbol	quantity	value	units
ϕ	porosity	.2	–
k	permeability	$1. \times 10^{-12}$	m^2
μ	viscosity	8.9×10^{-4}	Pa s
ρ	brine density	1.2×10^{3}	kg m^{-3}
g	gravity	9.80665	m s^{-2}
α_T	transverse dispersivity	2.	m
α_L	longitudinal dispersivity	20.	m
d	molecular diffusivity	0.	m^2 s^{-1}

FIRST-ORDER DECAY

Variable-Velocity Mixing

Next we apply T2DMR to a problem of dispersive mixing and radioactive decay of a passive tracer component in a flow field with a large-scale [O(100 m)] permeability heterogeneity located off-axis relative to the tracer source. The coupling in this problem is through hydrodynamic dispersion only. The permeability heterogeneity causes very slow velocities in the low-permeability region. These low velocities affect advective and dispersive mixing. The configuration is shown in Fig. 6, where the light stipple is the heterogeneity and the darker stipple is the region of injection of parent radionuclide. The heterogeneity is 100 times less permeable than the surrounding medium. With a pressure drop of $1. \times 10^5$ Pa across the 900-m wide domain, the average transit time across the domain is approximately 50 years. For this problem, we set the half-life of the parent to 500 years. The daughter is assumed stable. Parameters are presented in Table 3. In Fig. 7, we show the concentration of the parent at four times after injection. The parent is largely advected around the heterogeneity, but at steady state, clearly some parent has entered the low permeability heterogeneity. In Fig. 8, the daughter concentration at the same four times is shown. Daughter concentration is slow to build up in the low-permeability region but, remarkably, at steady state the maximum daughter concentration is located fully within the heterogeneity, completely off-axis from the parent maximum. It is apparent that over time, the parent component enters the heterogeneity by dispersion and advection. The residence time of the parent within the heterogeneity is relatively long; during this time, the parent decays to the daughter. The daughter is stable and does not decay, relying on dispersion and advection for its dilution. Only when the daughter concentration becomes quite large does its dispersive mixing balance its production by decay of parent. Details are presented in Oldenburg and Pruess (1995b).

Table 3. Parameters for the variable velocity radionuclide dispersion and decay problem.

symbol	quantity	value	units
ϕ	porosity	.2	–
k	permeability	$1. \times 10^{-12}$	m^2
μ	viscosity	8.9×10^{-4}	Pa s
α_T	transverse dispersivity	2.	m
α_L	longitudinal dispersivity	20.	m
d	molecular diffusivity	0.	m^2 s^{-1}
j	solute injection rate	1.6×10^{-6}	kg s^{-1}

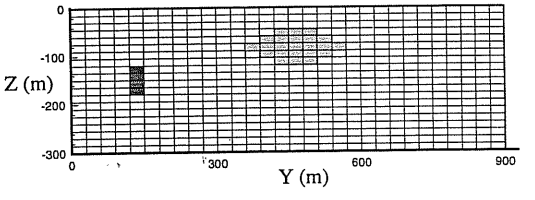

Fig. 6. Domain with permeability heterogeneity. Heavy stipple indicates the source grid blocks where parent is injected. Light stipple indicates the permeability heterogeneity where permeability is .01 of the background permeability.

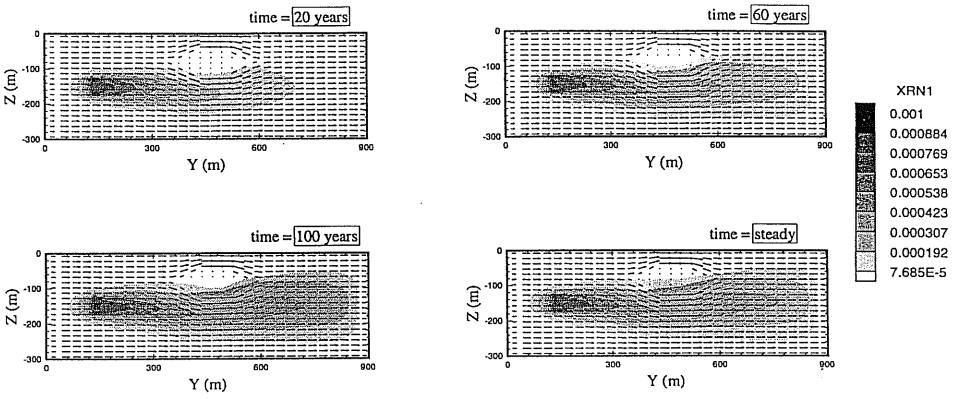

Fig. 7. Velocity and mass fraction of parent radionuclide component ($t_{1/2}$ = 500 years) in flow field with permeability heterogeneity at different times. Note the maximum concentration of parent occurs generally downstream from the grid blocks in which parent was injected.

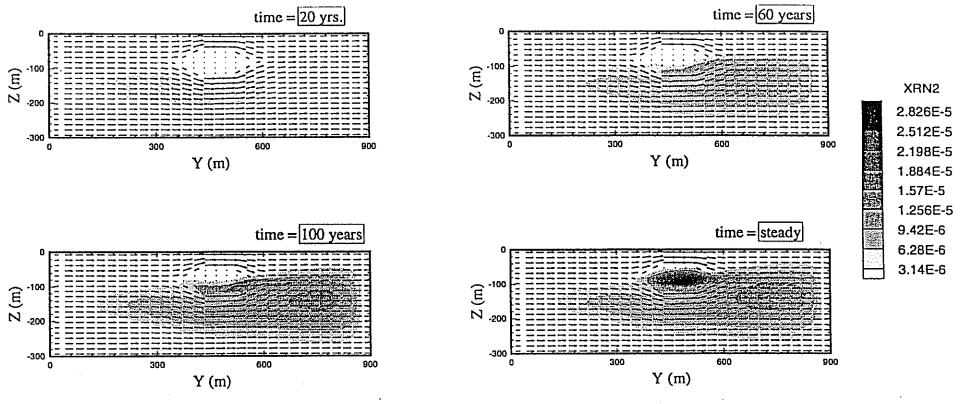

Fig. 8. Velocity and mass fraction of stable daughter radionuclide component in flow field with permeability heterogeneity at different times. Note the maximum concentration of daughter occurs within the permeability heterogeneity.

Salt-Dome Flow with First-Order Decay

Finally, we show an example calculation of the mixing of radioactive tracers in a more complicated flow field with a velocity gradient. The flow field itself comes from the strongly coupled salt-dome flow problem (Fig. 5). We inject passive radioactive components into the stippled grid block of Fig. 4c and we observe their distribution in time and space as they undergo decay and transport due to advection and hydrodynamic dispersion in the recirculating flow field.

In the steady-state salt-dome flow field, there is a weak recirculation near the right-hand wall caused by dense brine that has entered along the brine source but is too dense to be easily advected upward. Parent radionuclide is injected at a rate of 1.6e-6 kg/s in the grid block indicated in Fig. 9 by the stipple. The half-life is 50 years for the parent, and 250 years for the daughter. The concentration isopleths at t = 20, 60, 100, and 1400 years after injection are shown in Fig. 9. The daughter mass fraction is shown in Fig. 10. The maximum concentration of daughter shows a slight migration toward the lower boundary by t = 60 years. By t = 1400 years, the maximum daughter concentration lies in the weak recirculation in the lower right-hand corner. The maximum concentration of daughter has effectively moved down the velocity gradient and into the weak recirculation cell. The weak recirculation is a region of small advective velocity and long residence time analogous to the permeability heterogeneity of Fig. 8. Whereas one might expect the maximum daughter concentration to be found downstream from the maximum parent concentration, in fact the maximum daughter concentration lies within the recirculation.

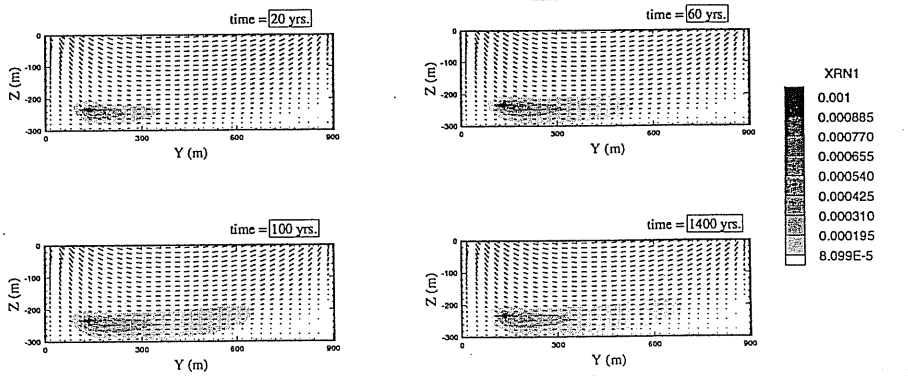

Fig. 9. Velocity and mass fraction of the parent ($t_{1/2}$ = 50 years) for salt-dome flow problem at different times.

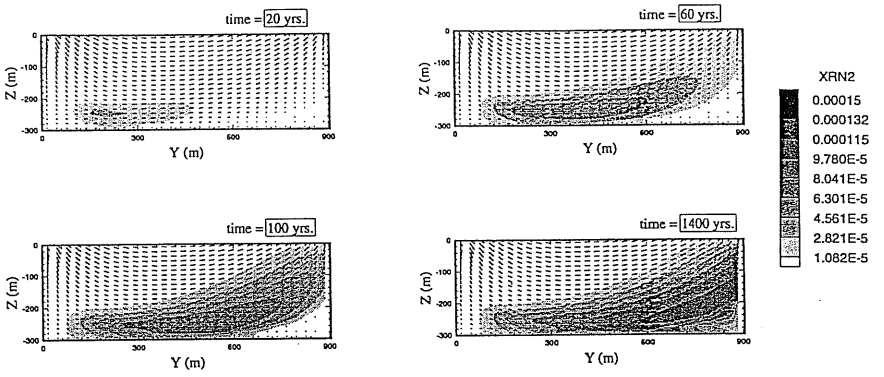

Fig. 10. Velocity and mass fraction of the daughter ($t_{1/2}$ = 250) years for salt-dome flow problem at different times. Note the maximum daughter concentration occurs within the weak recirculation in the lower right-hand corner.

CONCLUSIONS

Applications of T2DM and T2DMR to strongly coupled single-phase flow problems demonstrate the efficiency of the fully coupled solution technique in TOUGH2. For the Elder pure solutal convection problem, where strong coupling arises through density effects, T2DM is able to obtain answers similar to laboratory experimental results (Elder, 1967). For the salt-dome flow problem, where density and hydrodynamic dispersion couple the flow and transport, T2DM achieves verifiable steady-state answers that show a swept-forward flow field, a result fundamentally different from the best prior simulation results obtained using relative-change convergence criteria. T2MDR has been applied to coupled flow and transport of radioactive tracers undergoing decay in variable velocity flow fields. Our results indicate that daughter nuclides may reach their maximum concentrations not downstream from the parent source, but instead in regions of slow advective flow and corresponding long residence time.

Acknowledgments

This work was supported by the WIPP project, Sandia National Laboratories, and by the Office of Civilian Radioactive Waste Management, Yucca Mountain Site Characterization Project Office, U.S. Department of Energy, under contract No. DE–AC03–76SF00098. Computing support was provided by the Office of Basic Energy Sciences, U.S. DOE. We thank Stefan Finsterle and Yvonne Tsang for thoughtful reviews of an earlier draft.

Nomenclature

d	molecular diffusivity	$m^2\ s^{-1}$
g	acceleration of gravity	$m\ s^{-2}$
j	solute injection rate	$kg\ s^{-1}$
k	permeability	m^2
m	labels connected grid blocks	
M	mass accumulation term	$kg\ m^{-3}$
N	number of grid blocks	
NEQ	number of equations per grid block	
NK	number of mass components (species)	
NY	number of grid blocks in Y-direction	
NZ	number of grid blocks in Z-direction	
P	total pressure	Pa
q	source term	$kg\ m^{-3}\ s^{-1}$
R	residual	kg
t	time	years
V	volume	m^3
X	mass fraction	
Y	Y-coordinate	
Z	Z-coordinate (positive upward)	

Greek symbols

α	intrinsic dispersivity	m
ε	convergence criterion	
μ	dynamic viscosity	$kg\ m^{-1}\ s^{-1}$
ϕ	porosity	
ρ	density	$kg\ m^{-3}$
τ	tortuosity	

Subscripts and superscripts

b	brine
k	time-step index
L	longitudinal
m	indexes grid blocks connected to n
n	grid block index
p	Newton-Raphson iteration index
0	reference value
T	transverse
κ	mass components

References

Andersson, K., B. Grundfelt, D.P. Hodgkinson, B. Lindbom, and C.P. Jackson, *HYDROCOIN Level 1 Final Report: Verification of Groundwater Flow Models*, Swedish Nuclear Power Inspectorate (SKi), 1986.

Elder, J.W., Transient convection in a porous medium, *J. Fluid Mech.*,*27*(3), 609–623, 1967.

Herbert, A.W., Jackson, C.P., and Lever, D.A., Coupled groundwater flow and solute transport with fluid density strongly dependent on concentration, *Water Res. Res.*, *24* (10), 1781-1795, 1988.

Holzbecher, E., Numerische Modellierung von Dichteströmungen im porösen Medium, Technische Universität Berlin, *Mitteilung Nr. 117*, 1991.

Kipp, K.L., HST3D: A computer code for simulation of heat and solute transport in 3-D ground-water flow systems, *U.S. Geol. Surv., Water-resources Invest. Rep., 86-4095*, 1986.

Langer, M., Schneider, H., Kühn, K., The salt dome of Gorleben–target site for the German radioactive waste repository, pp. 57–66, in Witherspoon, P.A., *Proceedings of the Workshop W3B, 28th International Geological Congress*, Washington, D.C., July 1989, *Lawrence Berkeley Laboratory Report*, *LBL–29703*, January, 1991.

Oldenburg, C.M. and Pruess, K., A two-dimensional dispersion module for the TOUGH2 simulator, *Lawrence Berkeley Laboratory Report, LBL-32505*, 1993.

Oldenburg, C.M. and Pruess, K., T2DMR: Radionuclide transport for TOUGH2, *Lawrence Berkeley Laboratory Report, LBL- 34868*, 1994a.

Oldenburg, C.M. and Pruess, K., Numerical simulation of coupled flow and transport with TOUGH2: A verification study, *Lawrence Berkeley Laboratory Report, LBL- 35273*, 1994b.

Oldenburg, C.M. and Pruess, K., Dispersive transport dynamics in a strongly coupled groundwater-brine flow system, *Water Res. Res, 31*(2), 289–302, 1995a.

Oldenburg, C.M. and Pruess, K., Mixing with First-Order Decay in Variable Velocity Porous Media Flow, *Transport in Porous Media*, submitted, 1995b.

Pruess, K., TOUGH User's Guide, Nuclear Regulatory Commission, Report NUREG/CR-4645, June 1987 (also *Lawrence Berkeley Laboratory Report, LBL-20700*, Berkeley, California, June 1987).

Pruess, K., TOUGH2 - A General Purpose Numerical Simulator for Multiphase Fluid and Heat Flow, *Lawrence Berkeley Laboratory Report, LBL-29400*, Berkeley, California, May 1991).

Reeves, M., Ward, D.S., Johns, N.D., and Cranwell, R.M., Theory and implementation of SWIFT II, the Sandia Waste-Isolation Flow and Transport Model for Fractured Media, *Report No. SAND83-1159*, Sandia National Laboratories, Albuquerque, N.M., 1986.

The International Hydrocoin Project, Level 1: Code Verification , Rep. 71617, Organization for economic cooperation and development (OECD), Paris, France, 1988.

Voss, C.I., SUTRA: A finite-element simulation model for saturated-unsaturated fluid-density-dependent ground-water flow with energy transport or chemically-reactive single-species solute transport, *U.S. Geol. Surv. Water-resour. Invest. Rep.*, 84-4369, 409 pp., 1984.

Voss, C.I., and Souza, W.R., Variable density flow and solute transport simulations of regional aquifers containing a narrow freshwater-saltwater transition zone, *Water Res. Res., 23*(10), 1851–1866, 1987.